A HYBRID METHOD FOR LOW MACH NUMBER INTERNAL ACOUSTICS

[1]Morteza Bayati, [2]Mehran Tadjfar

Aerospace Department, Amirkabir University of Technology, Tehran, 15875-4413, Iran
Email : [1]mbayati@aut.ac.ir, [2]mtadjfar@aut.ac.ir

Abstract: A hybrid approach is proposed to extract the aeroacoustic noise generated by low Mach number internal flows. In many practical designs, often the sources of aeroacoustics distributed over non-compact distances. The traditional method for prediction of these regions, when an incompressible flow is adopted, it yields erroneous result. The present work by combining Curle's analogy with a boundary element method performs an appropriate approach for prediction of sound resulting from turbulence/body interaction for compact/non-compact regions. The validation of this method is performed by comparing the sound produced by the leapfrogging of two rectilinear filament vortices within an infinite two-dimensional straight duct by the acoustic field be obtained using tailored Green's function based on the non-evanescent duct modes. The flow field is obtained by integrating the reciprocal Biot-Sowart induction of the two spinning vortices. The sound is predicted in frequency domain applying the Curle/BEM approach, shows an excellent agreement with the reference solution.

Keywords: aeroacoustic, BEM, internal flow, infinite duct

I. INTRODUCTION

In many practical applications, sound is generated by interaction of turbulent flow with solid objects. In such cases, sound waves experience multiple reflections from solid objects. To predict the aeroacoustic field in these situations, an appropriate method is required to predict both directly propagated sound and scattered sound waves. More importantly, the employed method must avoid many simplification assumption often made about the geometry, compactness or frequency content of sound sources. The prediction of the acoustic performance as well as for analyzing the governing mechanism of aeroacoustics began more than fifty years ago, known as Lighthill [1] analogy. Lighthill's original work considered the propagation of acoustic waves from unbounded turbulent flows. Curle [2] extended Lighthill acoustic analogy with dipole nature to include the sound predicted by stationary, impermeable rigid surface immersed in the unsteady field. The work of Ffowcs Williams and Hawkings [3] allowed the impermeable rigid surface to be in arbitrary motion and resulting Doppler effects. The work of di Francescantanio [10] further extended this to allow the surface to be permeable.

In the present work there are considered with the noise generated by confined flows and its propagation with the analogy, by Davies and Ffowcs Williams [4]. They show that the acoustic efficiency of turbulent within a straight infinite duct varies with frequency, from a dipole like behavior below the cut-off frequency to free field quadrupole efficiency as soon as a few transverse modes are cut-on. Nelson and Morfey [5] and Peters and Hirschberg [6] studied to internal simple duct configurations such as diaphragm, contraction/ expansion. Low frequencies are often considered at traditional approaches, which present two advantages. Firstly the sources begin acoustically compact, it can be modeled by a point source. Secondly, for frequency below duct cut-off, one-dimensional Green's function can be employed to describe acoustic propagation. However, in many Industrial applications, often the sources of aeroacoustics distributed over non-compact distances. Furthermore, the spectrum of interest extends often beyond the transverse cut-off frequency, up to several KHz. The fact that the source is non-compact distance gives rise to difficulties such as discrimination between sound production and scattering effects. The compact body assumption is to neglect the scattering of sound produced by the body over itself [7]. Using an incompressible flow model for a non-compact configuration can yield quite erroneous result, as shown by Schram et al [8].

This work is aimed at the development of simulation methodology suitable for the prediction of aeroacoustic performance of flows confined in non-compact turbulent-body interaction region, i.e. high Helmholtz numbers He = kh = $2\pi fh/c_0$, such as heating, ventilating and air conditioning, automotive exhaust and pipe network with side branches, valves system. The conceptional differences in the simulation of sound generation and propagation are large enough to justify a treatment of the two as separate topics. The constraints like to this context imposed the choice of hybrid method. The unsteady turbulent flow is computed in duct to determine acoustic source terms, the latter being then propagated to produce the radiated noise. The implementation is analogy derived by Curl for prediction of the sound resulting from turbulent/body interactions. The pressure fluctuation that is involved in the dipole source term of Curle's analogy was decomposed Hydrodynamic pressure and acoustical pressure. The Hydrodynamic pressure can be resulted by an incompressible flow model and the latter component has to be computed in some way and added to the Hydrodynamic component in order to obtain correct result. A boundary element method (BEM) [9-10] is applied to model non-compactness effects. It consists of a discretization of the boundary integral solution of the Helmholtz equation assuming a free field Green's function.

The present paper includes some results of an aeroacoustical study of the leapfrogging of two rectilinear filament vortices within an infinite two-dimensional straight duct. Such a flow description being incompressible used to descript the acoustic sources. The acoustic results obtained using the Curle/BEM method, are compared to reference results using tailored Green's function.

II. BOUNDARY INTEGRAL FORMULATION OF CURLE'S ANALOGY

The inhomogeneous wave propagation equation is considered in the Fourier domain, which takes the form of the Helmholtz equation:

$$\nabla^2 \hat{P}_a + k^2 \hat{P}_a = \hat{q} \qquad (1)$$

In Eq. (1) $\hat{P}_a e^{i\omega t} = C_0^2 \hat{\rho} e^{i\omega t} = C_0^2 \rho'$, $k = \omega / C_0$ and $\hat{q} = \partial^2 T_{ij} / \partial x_i \partial x_j$ with $T_{ij} = \hat{T}_{ij} e^{i\omega t}$ is Lighthill's tensor. With some straightforward algebra, takes the following formula such as Curle's result but in the Fourier domain:

$$\hat{C}_0^2 \hat{\rho}(X,\omega) = \iiint_V \hat{T}_{ij} \frac{\partial^2 \hat{G}}{\partial y_i \partial y_j} d^3 y - \iint_{\partial V} \hat{P} \frac{\partial \hat{G}}{\partial y_i} n_i d^2 y \qquad (2)$$

In Eq. (2) the pressure $\hat{P}$ is the full pressure fluctuation (acoustic + hydrodynamic) and the Fourier domain free-field Green's function is $\hat{G} = \frac{1}{4} H_0^1(kr)$ with H_0^1 is Henkel's function of first kind and $r = ((x - x')^2 + (y - y')^2)^{1/2}$. In what follows, the hat notation, which indicate Fourier component, will be dropped for the sake of readability.

With convolute the Helmholtz equation with the free field Green's function yields:

$$C_0^2 \iiint_{V \backslash V_e} (\nabla^2 \rho G - \rho \nabla^2 G) d^3 y = \iiint_{V \backslash V_e} q G d^3 y + \iiint_{V \backslash V_e} C_0^2 \rho \delta(X - Y) d^3 y \qquad (3)$$

An exclusion volume V_ε which includes the listener's position X, was removed from the integration volume to the Green's theorem be applied in the domain which is free of the singularity of Green's function at X=Y. Therefore, the third integral of Eq. (3) is equal to zero. Applying Green's theorem and integrating by parts, Eq. (3) can be simplified as:

$$CP = \iiint_V T_{ij} \frac{\partial^2 G}{\partial y_i \partial y_j} d^3 y - \iint_{\partial V} P \frac{\partial G}{\partial n} d^2 y \qquad (4)$$

Where C is the solid angle is equal to 1 when X is within the volume, and equal to 1/2 when X lies over a smooth of the body and zero otherwhere.

As a corollary, the Eq. (4) can be seen as an implicit integral equation giving the pressure at any point of flow field, including body surface, provided the volumetric term is known.

An exact flow description satisfy Eq. (4), while an incompressible flow model only verify the same relation if the domain V is acoustically compact, i.e. if acoustical propagation is irrelevant. For a non-compact cases and incompressible flow model we decompose the wall pressure as the sum of a hydrodynamic and an acoustic components: $P = P_h + P_a$. Beside we decompose the integration domain in two parts, V_1 is localized around the collocation point X with dimensions compact and volume V_2 is defined as $V \backslash V_1$, and their boundaries ∂V_1 and ∂V_2. The hydrodynamic pressure over the compact domain V_1:

$$C(X) P_h(X) = \iiint_{V_1} T_{ij} \frac{\partial^2 G}{\partial y_i \partial y_j} d^3 y - \iint_{\partial V_1} P_h \frac{\partial G}{\partial n} d^2 y \qquad (5)$$

Subtracting Eq. (5) from Eq. (4) yields:

$$C(X)P_a(X) = -\iint_{\partial V} P_a \frac{\partial G}{\partial n} d^2 y + \iiint_{V2} T_{ij} \frac{\partial^2 G}{\partial y_i \partial y_j} d^3 y - \iint_{\partial V} P_h \frac{\partial G}{\partial n} d^2 y \qquad (6)$$

This integral implicit can be classically resolved using a boundary element method with Gaussian Quadrature method.

III. FLOW MODEL

An incompressible flow description is obtained by integrating the reciprocal Biot-Savart induction of the two leapfrogging vortices. The two-dimensional velocity field (u,v) is derived from the complex velocity potential: u- iv = dw/dz, where z = x + iy is the complex coordinate, in a coordinate system having the x-axis aligned with the duct symmetry axis. The calculation of the velocity field inside the duct and of the wall pressure field, induced by the two leapfrogging vortex filaments shown in Fig. 1, is performed in two steps. In the first step, the trajectories of the two vortices are integrated in time, by evaluating the velocity field induced at each vortex position by the other filament. The velocity field over the whole duct domain can then be obtained from the complex potential induced by the two vortices at each time step.

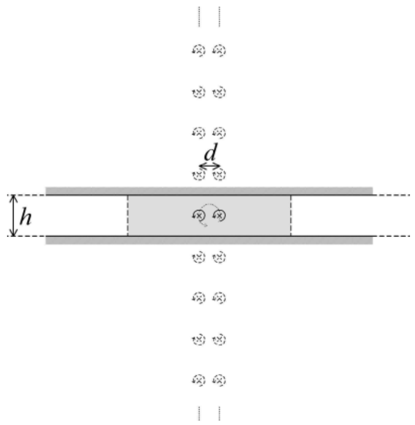

Fig. 1. Two rectilinear filament vortices

For a vortex filament placed within an infinite straight duct of height h, an infinite network of image vortices must be added to fulfill the non-penetration velocity boundary condition at the upper and lower walls located at the coordinates $z = ih/2$ and $z = -ih/2$. The resulting velocity potential due to the vortex n at the coordinate z_n is therefore:

$$\begin{aligned} \omega(z) = -\frac{i\Gamma}{2\pi} \{ & \log(z - z_n) \\ & -\log[z - (z_n + ih - 2iy_1)] + \log[z - (z_n - 2ih)] - \cdots \\ & -\log[z - (z_n - ih - 2iy_1)] + \log[z - (z_n + 2ih)] + \cdots \} \end{aligned} \qquad (7)$$

Where Γ is the circulation of each vortex. where the first line corresponds to the vortex filament within the duct, the second line sums the contributions of the vortex images due to the upper wall (including the image of this image by the lower wall, and so on), the third line sums the contributions of the image of the vortex due to the lower wall (including the image of this image due to the upper wall, and so on).

The duct height is h = 1 m, with a first cut-off frequency of 170 Hz. The vortex filaments are initially placed over the duct axis, separated by a distance h = 2 and a speed of sound $C_0 = 340\ \mathrm{ms}^{-1}$.

With solving the trajectories of the two vortices by time marching the equations for the velocity of each vortex filament m, induced by its own potential and the potential due to the other vortex n, accounting for their images:

$$\begin{aligned} u_m = -\frac{\Gamma}{4h} \Bigg\{ & \frac{\sin[\frac{\pi(y_m - y_n)}{h}]}{\cosh[\frac{\pi(x_m - x_n)}{h}] - \cos[\frac{\pi(y_m - y_n)}{h}]} \\ & + \frac{\sin[\frac{\pi(y_m + y_n)}{h}]}{\cosh[\frac{\pi(x_m - x_n)}{h}] + \cos[\frac{\pi(y_m + y_n)}{h}]} \\ & + \frac{\sin[2\pi y_m / h]}{1 + \cos[2\pi y_m / h]} \Bigg\} \end{aligned} \qquad (8)$$

$$\begin{aligned} v_m = -\frac{\Gamma}{4h} \Bigg\{ & \frac{-\sinh[\frac{\pi(x_m - x_n)}{h}]}{\cosh[\frac{\pi(x_m - x_n)}{h}] - \cos[\frac{\pi(y_m - y_n)}{h}]} \\ & + \frac{\sinh[\frac{\pi(x_m - x_n)}{h}]}{\cosh[\frac{\pi(x_m - x_n)}{h}] + \cos[\frac{\pi(y_m + y_n)}{h}]} \Bigg\} \end{aligned} \qquad (9)$$

For m, n = 1, 2 ($m \neq n$).

Integrating the unsteady Bernoulli equation along each wall yield the unsteady pressure distribution at the walls:

$$P_w = -\rho \left(\frac{\partial \Phi_w}{\partial t} + \frac{u_w^2}{2} \right) \qquad (10)$$

At every time step, velocity field corresponding to the azimuthal velocity within a radius $\delta = h/50$ from the vortex filament considered as:

$$u = -\frac{\Gamma}{2\pi} \frac{y}{x^2 + y^2 + \delta^2} \qquad (11)$$

$$v = \frac{\Gamma}{2\pi} \frac{x}{x^2 + y^2 + \delta^2}$$

Where the coordinate (x, y) are taken with respect to the vortex. A standard cell centered scheme is applied for calculation with regular spacing $\Delta x/h = \Delta y/h = 0.05$.

Fig. 2 illustrates, for a single time step, that the component T_{xy} = ρuv of Lighthill's tensor over the region of source field (-1.5 < x/h < 1.5) and the Fourier transform wall pressure fluctuation.

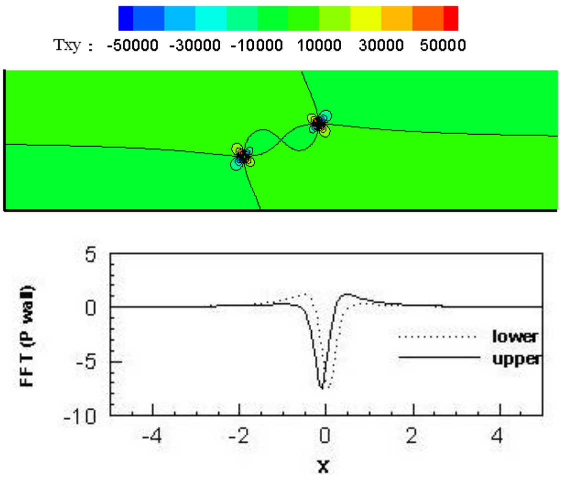

Fig. 2. Instantaneous Lighthill's tensors $T_{ij} = \rho_{\circ} u_i u_j$ and Temporal Fourier transformation of wall pressure fluctuations over both upper and lower walls.

Fig. 3 illustrates the Fourier transformation of Lighthill's tensor $T_{xy} = \rho_0 uv$ for $kh = 4.8$.

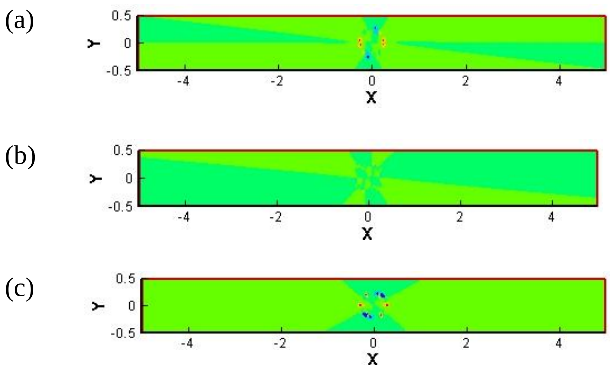

Fig. 3. Temporal Fourier transformation of Lighthill's tensors $T_{ij} = \rho_0 u_i u_j$ for $kh = 4.8$. (a) Txx, (b) Txy, (c) Tyy. Level of them is between -100…+100

Non-reflecting boundary condition is applied at both ends of the duct to permit comparison with the infinite duct reference solution. An acoustical impedance $Z = \rho_0 C_0$ boundary condition, which is anechoic for the plane wave propagation, is used at both ends of the duct model. The acoustic pressure has been solved for frequencies covering the range kh = 1…7, and compared with the exact solution obtained using the tailored Green's function from reference 8.

IV. SOUND EMITTED

The approach has been applied to the duct leapfrogging case. Fig. 4 show the sound field of dipole and quadrupole sources at kh = 4.8 from numerical solution. Fig. 5 show the sound field from quadrupole source alone at same kh and Fig. 6 show the sound field from dipole source alone at same kh. We observe that the dipoles contribute have more contribution from quadrupole at far from vortexes location. The important of quadrupole contribution is related to the relatively high Mach number, making the source region non-compact. Moreover, at this straight duct case the dipole merely represent mirrored reflection of the quadrupole, and have thus at most a similar acoustic efficiency.

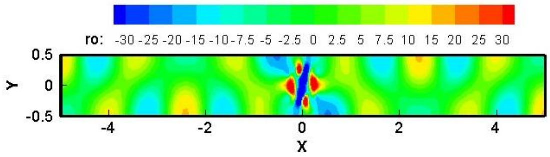

Fig. 4. Sound pressure field, dipole and quadrupole at kh = 4.8

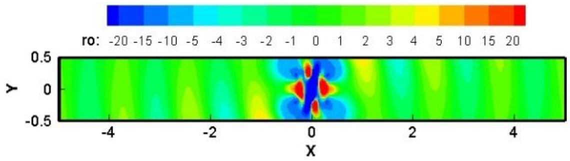

Fig. 5. Sound pressure field, quadrupole alone at kh = 4.8

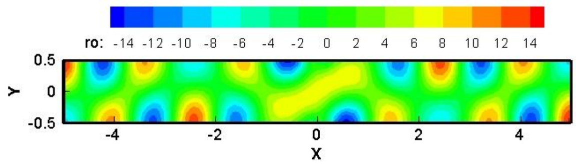

Fig. 6. Sound pressure field, dipole alone at kh = 4.8

Results at some frequencies, kh = 2.4, 3.2, 4.0, 4.8, 5.6, are displayed in Fig. 7. It shows amplitude of the sound pressure field at the domain at some harmonic frequencies and compare to Schram [7] data. The agreement is good for all frequencies except for fourth at kh = 3.2, where there are some discrepancies. This is maybe due to the inappropriate boundary condition $Z = \rho C$ to be most noticeable just above the cut-off frequencies of the duct. It can be concluded that a prediction with BEM method for infinite duct is not only meaningful below the cut-off frequency, but also for some frequencies within the interval between the first and second cut-off.

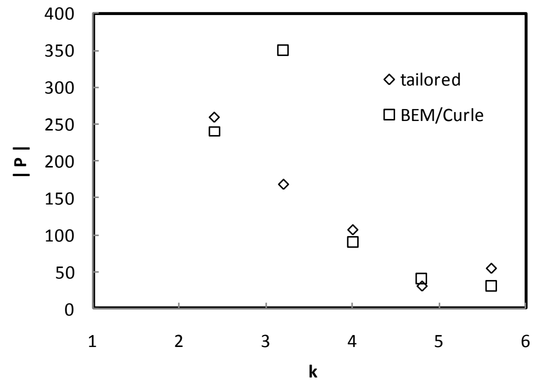

Fig. 7. Sound pressure amplitude

V. CONCLUSION

An approach combining the Boundary Element Method with Curle's analogy has been implemented. It has been applied to a benchmark for computational aeroacoustic: the sound produced by two leapfrogging vortex filament in an infinite two-dimensional duct. The results have good agreement between the numerical and reference data for all frequencies for which an approximate anechoic boundary condition was shown to be suitable. This hybrid method can solve the acoustic propagation in geometries of arbitrary extent and complex. In addition, it allows using an incompressible model of the flow field, which a compressible solvers face stiffness issues and converge slowly to a workable flow solution at low Mach numbers.

REFERENCES

[1] M. J. Lighthill, "On Sound Generated Aerodynamically. Part I. General Theory," Proc of the Royal Society of London, Series A. Mathematical and Physical Science, 1952, 211(1107), p. 564-587.

[2] N. Curle, "The Influence of Solid Boundaries upon Aerodynamic Sound," Proc of the Royal Society of London, Series A, 1955, 231, p. 505-514.

[3] J. E. Ffowcs Williams and D. L. Hawkings Sound Generation by Turbulence and Surfaces in Arbitrary Motion, Philosophical Transaction of the Royal Society, Series A, 1969, 264: 321-342.

[4] H. D. Davies and J. E. Ffowcs Williams, "Aerodynamic Sound Generation in a Pipe," Journal of Fluid Dynamics, 1968, 32(4), p. 765-778.

[5] P. A. Nelson and C. L. Morfey, " Aerodynamics Sound Prediction in Low Speed Flow Ducts," Journal of Sound and Vibration, 1981, 79(2), p. 263-289.

[6] M. C. A. M. Peters and A. Hirschberg, "Acoustically Induced Periodic Vortex Shedding at Sharp Edged Open Channel Ends: Simple Vortex Models," Journal of Sound and Vibration, 1993, 161(2), p. 281-299.

[7] C. Schram, " A boundary Element Extension of Curle's Analogy for Non-compact Geometries at Low Mach Numbers," Journal of sound and Vibration, 2009, 322, p. 264-281.

[8] C. Schram, J. Anthonie and A. Hirschberg, "Calculation of Sound Scattering Using Curle's Analogy for Non-compact bodies," Proc of the 11th AIAA/CEAS Aeroacoustics Conference and Exhibit, California, 2005, Number 2005-2836.

[9] D. I. Francescantonio, "A New Boundary Integral Formulation for the Prediction of Sound Radiation," Journal of Sound and Vibration, 1997, 202, p. 491-509.

[10] Y. Khalighi and D. Bodony, "Improve near-wall accuracy for solution of the Helmholtz equation using the boundary element method," CTR Annual Research Brief, 2006: 313-322.

◈◈◈